

Similarity theory of stellar models and structure of very massive stars

D.K. Nadyozhin^{1,2} T.L. Razinkova²

¹*Max-Planck-Institut für Astrophysik, Garching, Germany*

²*A.I. Alikhanov Institute for Theoretical and Experimental Physics,
Moscow, Russia*

Abstract

The similarity theory of stellar structure is used to study the properties of very massive stars when one can neglect all the sources of opacity except for the Thomson scattering. The dimensionless internal structure of such stars is practically independent of the energy generation law. It is shown that the mass-luminosity relation can be approximated by an analytical expression which is virtually universal regarding the chemical composition and energy generation law. A detailed comparison with the Eddington standard model is given. The application of the obtained results to the observations of massive stars is briefly discussed.

1 Introduction

The similarity theory of stellar structure was a powerful tool to understand the properties of stellar models during the pre-computer era of their study. Suffice it to mention a theoretical explanation of the mass-luminosity and mass-radius relations (Biermann, 1931; Strömgren, 1936; Sedov, 1959). For years the similarity theory remains to be useful for the interpretation of various aspects of stellar structure (Schwarzschild, 1958; Chiu, 1968; Cox, Guili, 1968; Dibai, Kaplan, 1976; Kippenhahn, Weigert, 1990).

Here, first we describe the similarity theory of stellar structure as a boundary-value problem formulated by Imshennik and Nadyozhin (1968).

Then we discuss the structure of chemically homogeneous stars of so large a mass that the opacity can be considered as being due to the Thomson scattering alone. Such an approximation is believed to be adequate for still hypothetical Pop III stars and for a number of observed luminous stars — e.g., massive O-stars, Wolf-Rayet stars, and some specific stars like η Car, and the Pistol star. A special consideration is given to the comparison with the Eddington standard model.

2 Similarity theory of stellar models

Let us consider a spherical star in hydrostatic and thermal equilibrium. If the pressure P is contributed by perfect gas P_g and black body radiation P_r and the rate of energy generation ε and opacity κ are the power functions of the temperature T and density ρ then the structure of the star is described by the following set of differential equations:

$$\frac{dP}{dr} = -\rho \frac{Gm}{r^2}, \quad (1)$$

$$\frac{dm}{dr} = 4\pi r^2 \rho, \quad (2)$$

$$\frac{dL}{dr} = 4\pi r^2 \rho \varepsilon, \quad (3)$$

$$\frac{dT}{dr} = \begin{cases} -\frac{\rho T}{P} \frac{Gm}{r^2} \nabla_A, & \nabla_r \geq \nabla_A, & \nabla_A = \left(\frac{\partial \log T}{\partial \log P} \right)_S, \\ -\frac{\rho T}{P} \frac{Gm}{r^2} \nabla_r, & \nabla_r \leq \nabla_A, & \nabla_r = \frac{3\kappa L P}{16\pi c a T^4 Gm}, \end{cases} \quad (4)$$

$$P = P_g + P_r = \frac{k}{m_u} \frac{1}{\mu} \rho T + \frac{1}{3} a T^4, \quad (5)$$

$$\beta = \frac{P_g}{P}, \quad \beta^{-1} = 1 + \mu \frac{a m_u}{3k} \frac{T^3}{\rho}, \quad \nabla_A = \frac{2(4 - 3\beta)}{32 - 24\beta - 3\beta^2}, \quad (6)$$

$$\kappa = \kappa_0 \rho^\alpha T^{-\nu}, \quad \varepsilon = \varepsilon_0 \rho^\delta T^\eta, \quad (7)$$

where β is the ratio of the gas pressure to the total one; G , k , and a are the gravitational, Boltzmann, and radiation density constants, respectively; m_u is the atomic mass unit and c is the speed of light. The mean molecular mass μ and the coefficients κ_0 and ε_0 depend on composition.

The above equations should meet the boundary conditions:

$$\text{Center } r = 0 : \quad m = 0, \quad L = 0, \quad (8)$$

$$\text{Surface } r = R : \quad P = 0, \quad \rho = 0, \quad m = M. \quad (9)$$

The conditions (8) tell that there is neither point mass nor point source of energy in the center of the star. The conditions (9) at stellar surface state that both the pressure and density vanish there and the mass m must be equal to the total mass M specified for the star. The stellar radius R is to be obtained as a result of the solution of Eqs. (1)–(7), i.e. R is an eigenvalue of the problem. Simultaneously, the solution gives the luminosity of the star $L_0 \equiv L(R)$.

Assuming that the chemical composition and, consequently, μ , κ_0 , and ε_0 are constant throughout the star, one can reduce the above equations to a dimensionless form by measuring the physical quantities in the following set of units (Schwarzschild, 1958):

$$r \rightarrow R, \quad m \rightarrow M, \quad L \rightarrow L_0, \quad (10)$$

$$T \rightarrow \mu \frac{m_u GM}{k R} \equiv T_0, \quad P \rightarrow \frac{GM^2}{4\pi R^4} \equiv P_0, \quad \rho \rightarrow \frac{M}{4\pi R^3} \equiv \rho_0.$$

Introducing the following dimensionless variables

$$x = r/R, \quad q = m/M, \quad l = L/L_0, \quad p = P/P_0, \quad \sigma = \rho/\rho_0, \quad t = T/T_0, \quad (11)$$

one can rewrite Eqs. (1)–(9) in the form (Imshennik, Nadyozhin, 1968):

$$\frac{dp}{dx} = -\frac{\sigma q}{x^2}, \quad (12)$$

$$\frac{dq}{dx} = x^2 \sigma, \quad (13)$$

$$\frac{dl}{dx} = C_1 x^2 \sigma^{1+\delta} t^\eta, \quad (14)$$

$$\frac{dt}{dx} = \begin{cases} -\frac{q\sigma t}{x^2 p} \nabla_A, & \nabla_r \geq \nabla_A, \quad \nabla_A(\beta) = \frac{2(4-3\beta)}{32-24\beta-3\beta^2}, \\ -\frac{q\sigma t}{x^2 p} \nabla_r, & \nabla_r \leq \nabla_A, \quad \nabla_r = C_2 \frac{pl\sigma^\alpha}{qt^{4+\nu}}, \end{cases} \quad (15)$$

$$p = \sigma t + B t^4, \quad \beta^{-1} = 1 + B \frac{t^3}{\sigma}, \quad (16)$$

where all the parameters are gathered in the three dimensionless constants:

$$C_1 = \frac{1}{(4\pi)^\delta} \left(\frac{Gm_u}{k} \right)^\eta \mu^\eta M^{1+\delta+\eta} \frac{\varepsilon_0}{L_0 R^{3\delta+\eta}}, \quad (17)$$

$$C_2 = \frac{3(4\pi)^{-\alpha}}{64\pi^2 ac} \left(\frac{k}{Gm_u} \right)^{4+\nu} \mu^{-4-\nu} M^{\alpha-3-\nu} \frac{\kappa_0 L_0}{R^{3\alpha-\nu}}, \quad (18)$$

$$B = \frac{4\pi a}{3G} \left(\frac{Gm_u}{k} \right)^4 (\mu^2 M)^2 = 0.78096 (\mu^2 M / M_\odot)^2. \quad (19)$$

The dimensionless boundary conditions become:

$$\text{Center } x = 0 : \quad q = 0, \quad l = 0, \quad (20)$$

$$\text{Surface } x = 1 : \quad p = 0, \quad t = 0, \quad l = 1, \quad q = 1. \quad (21)$$

Thus, we have now six boundary conditions for four first order differential equations (12)–(15). This means that for every given B (or $\mu^2 M$) the constants C_1 and C_2 can have only quite certain values (eigenvalues) in order that the solution of *four* differential equations would satisfy to *six* boundary conditions. The solution itself as well as C_1 and C_2 depend only on $\mu^2 M$ and the exponents $\alpha, \nu, \delta, \eta$: $C_{1,2} = C_{1,2}(\mu^2 M, \alpha, \nu, \delta, \eta)$.

Equations (12)–(16) can be solved by standard methods. For the calculations described in the next section, we have used the following approach. Having chosen some trial values of C_1 and C_2 and integrating Eqs. (12)–(16) numerically from the surface [$x = 1$, boundary conditions (21)] inward to some value $x = x_f$ ($0 < x_f < 1$), one obtains a set of four quantities $\{p(x_f), q(x_f), l(x_f), t(x_f)\}$ as functions of C_1 and C_2 . Then integrating these equations again from the center [$x = 0$, boundary conditions (20)] with the same C_1 and C_2 and trial values $p(0) = p_c$ and $t(0) = t_c$ outward to x_f one obtains a similar set of quantities that depends now on C_1, C_2, p_c , and t_c . Since $p(x), q(x), l(x)$, and $t(x)$ must be continuous throughout the star, both the sets have to coincide at $x = x_f$. One can organize an iterative process for four unknown parameters C_1, C_2, p_c , and t_c to find such their values that would ensure the desired continuity of four variables p, q, l , and t at $x = x_f$. Of course, the result does not depend on x_f but the convergence domain of the iterations does.

As soon as C_1 and C_2 are found, one can easily derive the luminosity L_0 and radius R from Eqs. (17) and (18) which represent the mass-radius and mass-luminosity relation, respectively.

3 Structure of very massive stars

In this section, the above similarity theory is employed to describe the structure of very massive stars. In this case the opacity is dominated by the Thomson scattering and one can assume $\alpha = 0$, $\nu = 0$, and $\kappa = \kappa_0 = 0.2(1 + X)$ cm²/g (X is the mass fraction of hydrogen).

The mass-luminosity relation [Eq. (18)] can be converted into the form

$$L_0 = \frac{64\pi^2 ac}{3\kappa_0} \left(\frac{Gm_u}{k} \right)^4 \mu^4 M^3 C_2(\mu^2 M, \delta, \eta). \quad (22)$$

All the models with physically reasonable values of the energy generation temperature exponent (i.e., $\eta \geq 4$) considered below have convective cores and radiative outer envelopes. Using Eqs. (12) and (15) and boundary conditions (21), one can find that C_2 is simply connected with $\beta_s(\mu^2 M, \delta, \eta)$ — the value of the parameter β at stellar surface:

$$1 - \beta_s = 4 B C_2. \quad (23)$$

Now the mass-luminosity relation can be reduced to

$$L_0 = L_{\text{Ed}}(1 - \beta_s), \quad (24)$$

where the Eddington critical luminosity L_{Ed} is given by

$$L_{\text{Ed}} \equiv \frac{4\pi cGM}{\kappa_0} = \frac{6.483 \times 10^4}{1 + X} \frac{M}{M_\odot} L_\odot. \quad (25)$$

Using the Runge–Kutta method with automatic control of accuracy for solving Eqs. (12)–(16) from stellar surface down to x_f and from center up to x_f , we have calculated a large number of models for a wide interval of the parameter $\mu^2 M$ ($0 \leq \mu^2 M \leq 4,000 M_\odot$). Typically, the values $x_f \approx 0.1–0.3$ are the best for the iterations to converge. The convergence domain, however, turned out to be rather narrow at least for the Newton–Raphson iteration scheme used in our calculations. So, when calculating a sequence of such models one has to change $\mu^2 M$ at most by a few percents in order to ensure the convergence.

Table 1 presents the most important properties of several selected models. Note that for the sake of a better perception we use hereafter for dimensionless quantities the same designations as for dimensional ones. The first row

Table 1: Structural properties of selected models

$\mu^2 M$	0	10	30	100	300	1000	4000
$\log_{10} C_1^*$	1.6347	3.4318	5.8102	8.8083	11.768	15.281	19.622
$\log_{10} C_1^\dagger$	2.1212	5.8346	10.615	16.602	22.509	29.523	38.199
$\log_{10} C_1^\spadesuit$	-0.4145	0.0220	0.5988	1.2961	1.9789	2.8051	3.8511
$\log_{10} C_2$	-3.2981	-3.5181	-3.9842	-4.7533	-5.5839	-6.5626	-7.7304
ρ_c	59.34	60.20	65.05	79.97	98.95	119.4	137.5
P_c	45.55	43.95	46.43	58.41	75.32	94.78	112.8
T_c	0.7677	0.5816	0.4097	0.2630	0.1699	0.1014	0.0539
∇_{rc}^*	2.459	3.249	4.525	5.806	6.588	6.992	7.266
φ_c	-3.428	-3.389	-3.421	-3.602	-3.821	-4.034	-4.204
β_c	1	0.7967	0.5739	0.3601	0.2232	0.1278	0.0657
β_{conv}	1	0.8671	0.6689	0.4294	0.2600	0.1429	0.0704
β_s	1	0.9053	0.7085	0.4489	0.2673	0.1451	0.0709
r_{conv}	0.2832	0.3903	0.5107	0.6264	0.7077	0.7771	0.8380
m_{conv}	0.3120	0.5691	0.8063	0.9412	0.9823	0.99531	0.99895
$L_{\text{conv}}^\spadesuit$	0.7810	0.9799	0.9991	1.0000	1.0000	1.0000	1.0000
ρ_{conv}	31.39	16.02	5.985	1.661	0.5056	0.1429	0.0379
P_{conv}	15.76	5.830	1.446	0.2540	0.05324	0.01049	0.00184
T_{conv}	0.5022	0.3157	0.1616	0.06564	0.02736	0.01036	0.00342

* CNO-cycle ($\delta = 1, \eta = 16$), † 3α -reaction ($\delta = 2, \eta = 30$), $^\spadesuit$ pp-chain ($\delta = 1, \eta = 4$)

of Table 1 gives $\mu^2 M$ with M measured in M_\odot . The next three rows are the C_1 -values for three modes of energy generation: the CNO-cycle, 3α -reaction, and pp-chain. The fifth row gives the C_2 -values. The next six rows relate to the central dimensionless values of density ρ_c , pressure P_c , temperature T_c , radiative temperature gradient ∇_{rc} , gravitational potential φ_c (in the units GM/R), and ratio β_c of the gas pressure to the total one. The next two rows contain β_{conv} and β_s at the convective core boundary and at stellar surface, respectively. Finally, the last six rows present the dimensionless values of radius, mass, luminosity, density, pressure, and temperature at the convective core boundary.

The calculated sequences of one-parametric (depending on $\mu^2 M$) dimensionless models have so large convective cores that the major part of thermonuclear energy turns out to be released within the core. Therefore, $L(r)$ becomes almost equal to the luminosity L_0 everywhere outside the convec-

tive core. For such a strong dependence of the energy generation on temperature as in the CNO-cycle ($\eta = 16$) and in 3α -reaction ($\eta = 30$), one can with a high accuracy assume $l(x) = 1$ in Eq. (15). Consequently, Eq. (14) for $l(x)$ proves to be disentangled from other equations (12), (13), (15), and (16). Now one can calculate the overall stellar structure by solving a truncated eigenvalue problem that pays no attention to the law of energy generation and considers the constant C_2 as a single eigenvalue parameter involved. In particular, the resulting C_2 -eigenvalue, and consequently L_0 [Eq. (22)], as well as the dimensionless stellar structure do not depend on the exponents δ and η . Such a truncated model is actually the point-source model with the Thomson opacity and allowance for the radiation pressure that was first calculated by Henrich (1943) within a limited range of stellar mass ($0 \leq \mu^2 M \leq 119$). Our numerical results are in excellent agreement with his $\sim 1\%$ accurate calculations.

When C_2 and the dimensionless functions $\sigma(x)$ and $t(x)$ are already known from the solution of the truncated problem one can find the constant C_1 and spatial distribution of the dimensionless luminosity $l(x)$:

$$C_1 = \left[\int_0^1 x^2 \sigma^{1+\delta} t^\eta dx \right]^{-1}, \quad l(x) = C_1 \int_0^x x^2 \sigma^{1+\delta} t^\eta dx. \quad (26)$$

If the energy generation is an arbitrary (but still strongly varying with temperature) function: $\varepsilon = \varepsilon(\rho, T)$, then instead of C_1 one has to consider the stellar radius R as an eigenvalue that can be found from the equation

$$L_0 = M \int_0^1 x^2 \sigma(x) \varepsilon \left[\frac{M}{4\pi R^3} \sigma(x), \mu \frac{m_u}{k} \frac{GM}{R} t(x) \right] dx, \quad (27)$$

where for given M and composition the luminosity L_0 is determined by the C_2 -value obtained for the truncated model.

The structural properties of the models presented in Table 1 correspond to three modes of energy generation: the CNO-cycle, 3α -reaction, and pp-chain. For the CNO-cycle and 3α -reaction, the dimensionless luminosity L_{conv} at the convective core boundary is equal to 1.0000 for all the values of $\mu^2 M$. The same is true for the pp-chain when $\mu^2 M \gtrsim 30$. All other parameters in Tables 1 and 2, except for C_1 and ∇_{rc} , prove to be the same for the CNO-cycle and 3α -reaction, and at $\mu^2 M \gtrsim 30$ for the pp-chain as well. Practically, one can consider only the interval $0 \leq \mu^2 M \lesssim 10$ as exhibiting slight differences for the pp-chain shown in Figures 4, 5, 6 below.

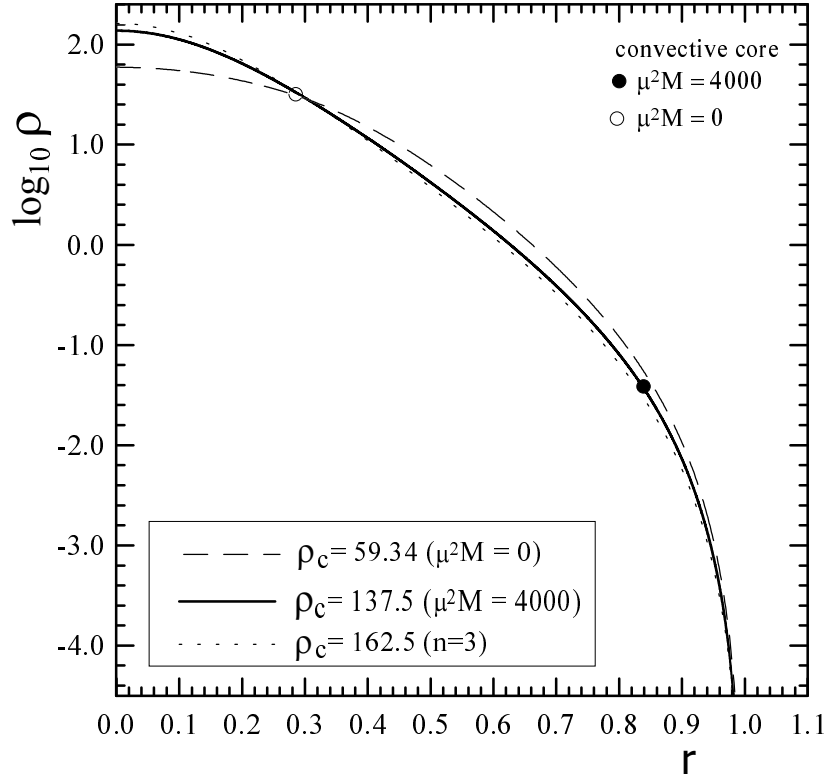


Figure 1: Density versus radius in the units defined by Eqs. (10) for $\mu^2 M = 0$ (dashed line), 4000 (full line) and for a polytropic model ($n = 3$, dotted line). The boundaries of the convective core are indicated for $\mu^2 M = 0$ and 4000.

This concerns also the mass-luminosity relation. More specifically, for $\eta = 4$: $\log_{10} C_2 = -3.516$ and -3.285 at $\mu^2 M = 10$ and 0 , respectively.

The constant C_1 and central value of the logarithmic radiative temperature gradient $\nabla_{rc} = C_1 C_2 p_c \sigma_c^\delta t_c^{\eta-4}$ strongly depend on the energy generation law. The ∇_{rc} values for the CNO-cycle in Table 1 demonstrate that even for low masses ($\mu^2 M \lesssim 1$) when one can neglect the radiation pressure, there is still a good excess of ∇_{rc} over ∇_A ($0.25 \leq \nabla_A \leq 0.4$) to drive the adiabatic convection along stellar core. For the 3α -reaction, the excess is much larger: $\nabla_{rc} = 11.05$ for $\mu^2 M = 0$. However for the pp-chain we have $\nabla_{rc} = 0.594$ — the value exceeding the adiabatic gradient only by a factor of 1.5 ($\nabla_{Ac} = 0.4$ for $\mu^2 M \approx 0$). This happens because the exponent $\eta = 4$ is not very far from a critical value of $\eta \approx 2 - 3$ necessary to ensure the existence of the

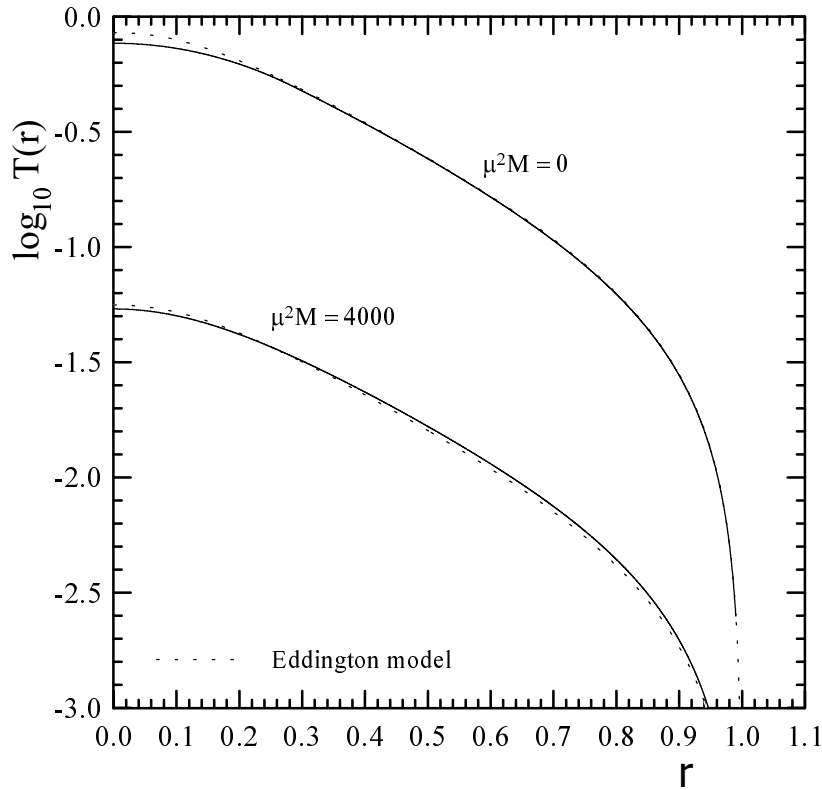


Figure 2: Temperature versus radius in the units defined by Eqs. (10) for $\mu^2 M = 0$ and 4000. The Eddington model is shown by the dotted lines.

convective core (Cowling, 1934; Naur, Osterbrock, 1953).

Figures 1 and 2 show the density and temperature versus radius for two extreme values of $\mu^2 M$ in the case of the CNO-cycle and 3α -reaction. With a high accuracy these two modes of energy generation result in only one model for every given $\mu^2 M$ (see the discussion above).

It is instructive to compare the results with the Eddington standard model (Eddington, 1926) that at constant opacity corresponds to a constant rate of energy generation: $\varepsilon = \varepsilon_0$ ($\eta = 0$, $\delta = 0$). In this case $C_1 = 1$ as it immediately follows from Eq. (26). Then, it is easy to make sure that β is to be constant inside such a model. As a result, the pressure turns out to be connected with density along the radius by a power law:

$$P = K \rho^{4/3}, \quad K \equiv \frac{k}{m_u \mu} \left[\frac{3k}{am_u \mu} \frac{1 - \beta}{\beta^4} \right]^{1/3} = \text{const}. \quad (28)$$

Thus, the standard model is nothing else than a polytropic gas sphere of

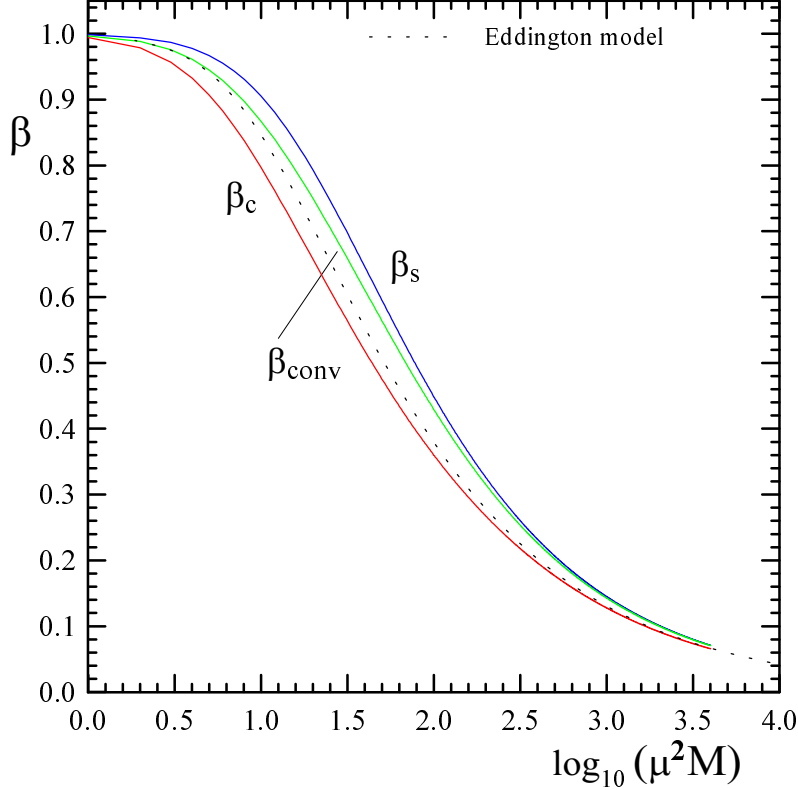


Figure 3: The ratios of the gas pressure to the total one, β , at the center β_c , the convective core boundary β_{conv} , and the surface β_s as functions of $\mu^2 M$ (M is in M_\odot). A dotted curve corresponds to the Eddington standard model [Eq. (29)].

index $n = 3$. The value of β proves to be uniquely connected with the mass M by the following equation (Chandrasekhar, 1939):

$$\frac{1 - \beta}{\beta^4} = 0.01607 G^3 \left(\frac{m_u}{k}\right)^4 (\mu^2 M)^2 = 2.994 \times 10^{-3} \left(\mu^2 \frac{M}{M_\odot}\right)^2. \quad (29)$$

The constant C_2 as a function of $\mu^2 M$ and the mass-luminosity relation for the standard model are determined by Eqs. (23) and (24) with β_s being substituted for β from Eq. (29). It is easy to verify that the Eddington standard model has no convective core at all — it is convectively stable for any $\mu^2 M$.

According to Fig. 3, β increases from the stellar center up to the surface: $\beta_c < \beta_{\text{conv}} < \beta_s$, the Eddington β always remaining between β_c and β_{conv} .

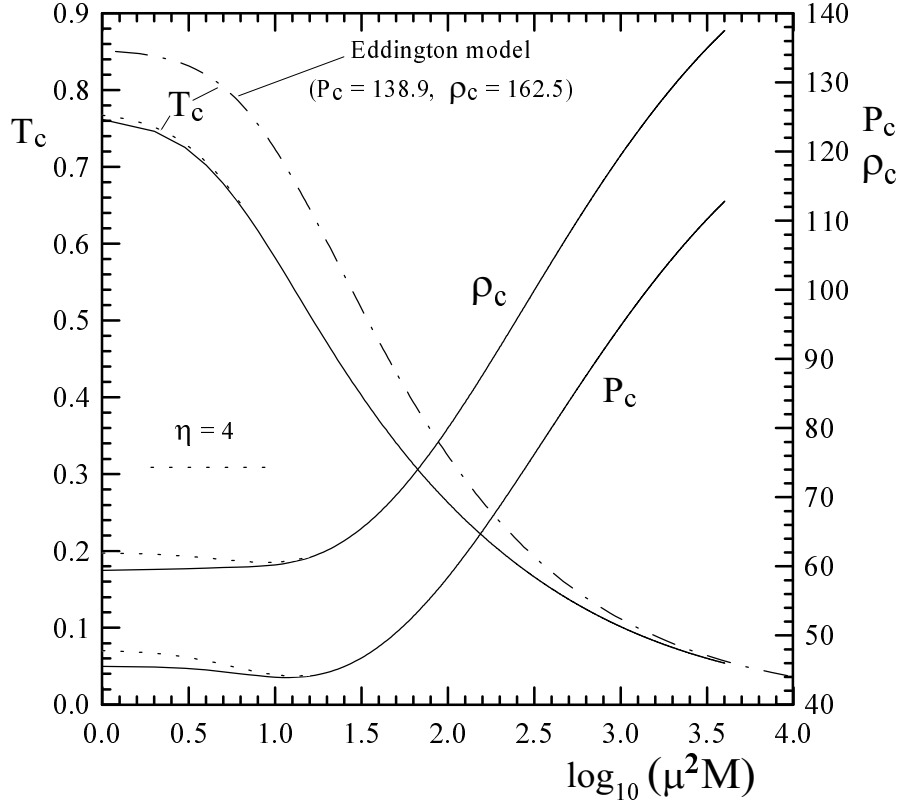


Figure 4: The dimensionless central pressure P_c , density ρ_c (right vertical axis), and temperature T_c (left vertical axis) as functions of $\mu^2 M$ (M is in M_\odot).

Figure 4 shows the central pressure P_c , density ρ_c and temperature T_c as functions of $\mu^2 M$. At $\mu^2 M \lesssim 10$, these quantities for the pp-chain (dotted lines) only slightly differ from those for the CNO-cycle and 3α -reaction (solid lines). The broken line represents T_c for the Eddington model for which P_c and ρ_c are independent of $\mu^2 M$: $P_c = 138.9$, $\rho_c = 162.5$ (polytrope $n = 3$!).

Figure 5 shows how the dimensionless radius of the convective core r_{conv} , the value of β at the convective core boundary β_{conv} , and the mass above the convective core ($1 - m_{\text{conv}}$) depend on $\mu^2 M$. At $\mu^2 M \gtrsim 40$, the convective core contains more than 85% of stellar mass. One can approximate m_{conv} (for

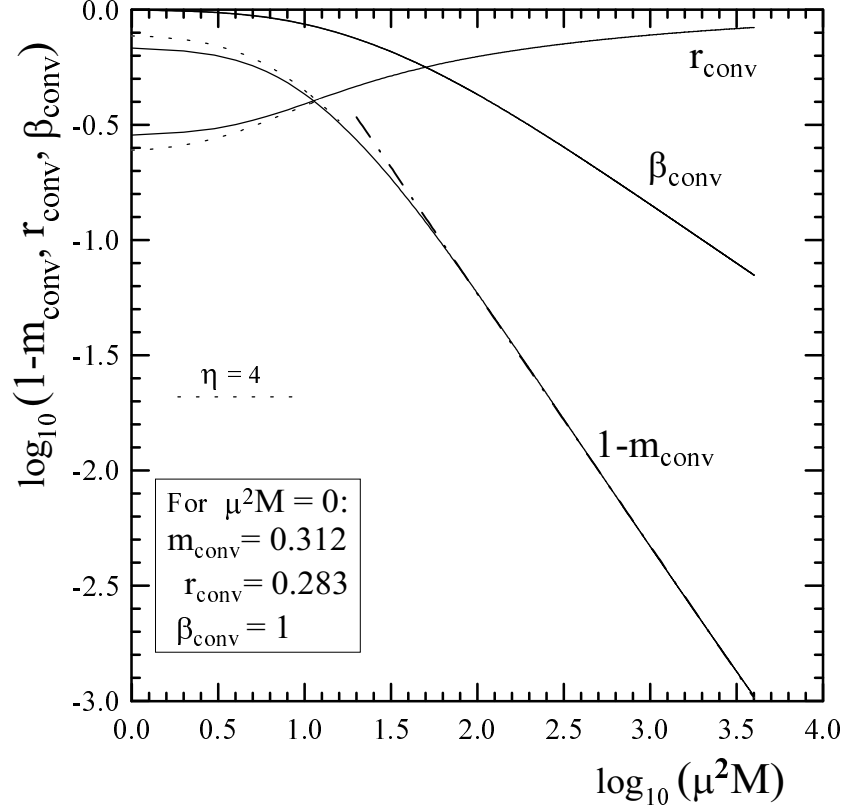


Figure 5: The convective core boundary characteristics as functions of $\mu^2 M$ for the CNO-cycle and 3α -reaction (solid lines) and pp-chain (dotted lines). The values for the CNO-cycle and 3α -reaction at $\mu^2 M = 0$ are shown explicitly.

all the three energy generation modes!) by the following asymptotic relation (a straight broken line in Fig. 5):

$$m_{\text{conv}} = 1 - 9.075 (\mu^2 M)^{-1.095}, \quad \mu^2 M \gtrsim 40. \quad (30)$$

Since the constant C_1 strongly depends on the energy generation mode (Table 1), it is useful to introduce a modified constant C_{1m} :

$$C_{1m}(\mu^2 M) \equiv (\mu^2 M)^{\frac{\delta+\eta}{3\delta+\eta}} [(1 - \beta_s) C_1]^{-\frac{1}{3\delta+\eta}}, \quad (M \text{ in } M_\odot). \quad (31)$$

Now, using Eq. (24) for L_0 we can obtain the following expression for stellar

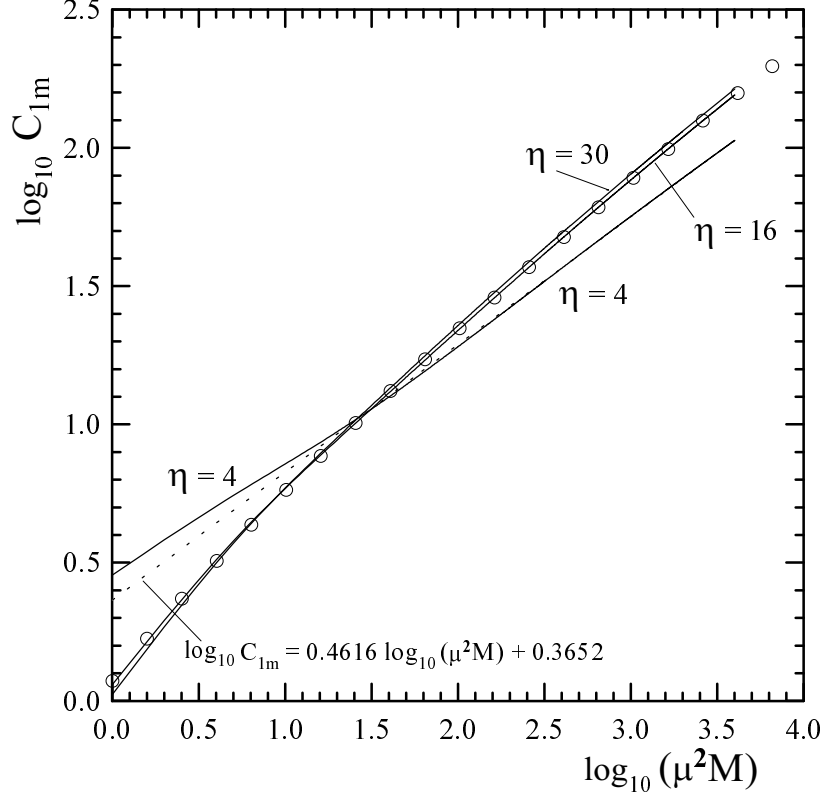


Figure 6: The modified constant C_{1m} as a function of $\mu^2 M$ for the CNO-cycle, 3α -reaction and pp-chain. The open circles and dashed line show polynomial fits.

radius as a function of $\mu^2 M$ and composition:

$$\log R = \log C_{1m} + \log D + \log S, \quad (R \text{ in } R_{\odot}), \quad (32)$$

where

$$\begin{aligned} \log D &= \frac{1}{3\delta + \eta} \log[0.2(1 + X)\xi] - \frac{2\delta + \eta}{3\delta + \eta} \log \mu, \\ \log S &= \frac{\eta}{3\delta + \eta} \log\left(\frac{Gm_u}{k}\right) - \frac{\delta + 1}{3\delta + \eta} \log(4\pi) \\ &\quad + \frac{1}{3\delta + \eta} \log\left(\frac{\varepsilon_{00}}{cG}\right) + \frac{\delta + \eta}{3\delta + \eta} \log M_{\odot} - \log R_{\odot}, \\ \xi &\equiv X^2 \text{ (pp-chain)}, \quad XX_{\text{CNO}} \text{ (CNO-cycle)}, \quad Y^3 \text{ (3}\alpha\text{-reaction)}. \end{aligned}$$

Here, the dependences of ε_0 on the mass fractions of hydrogen X , the CNO-isotopes X_{CNO} , and helium Y are shown explicitly ($\varepsilon_0 = \varepsilon_{00} \xi$). For large values of η , $C_{1\text{m}}$ becomes independent of the energy generation mode — compare the CNO ($\eta = 16$) and 3α ($\eta = 30$) curves in Fig. 6. Both the $C_{1\text{m}}$ can be approximated by a single polynomial shown by open circles in Fig. 6:

$$y = 0.0720052 + 0.782547x - 0.120854x^2 + 0.0295923x^3 - 0.0030574x^4, \quad (33)$$

where $y \equiv \log_{10} C_{1\text{m}}$ and $x \equiv \log_{10} (\mu^2 M)$. A fit for the pp-chain ($\eta = 4$) is shown in Fig. 6 by a dashed line that gives a good accuracy for $\mu^2 M \gtrsim 10$.

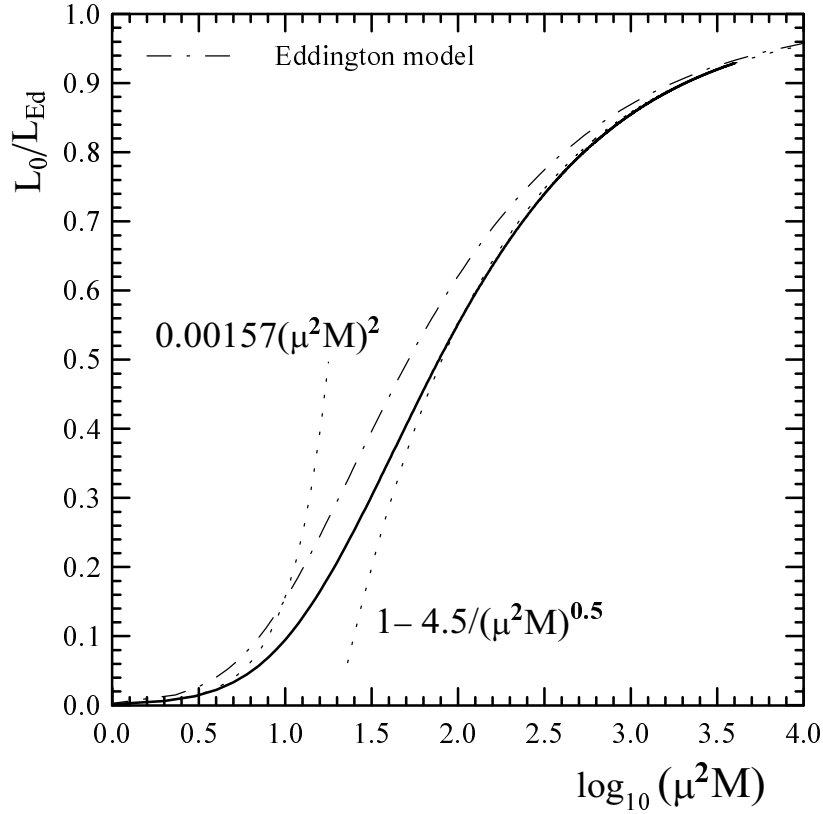


Figure 7: The normalized mass-luminosity relation [Eq. (24)]. Dotted curves indicate asymptotics for small and large $\mu^2 M$ -values. The Eddington model is shown by a broken line.

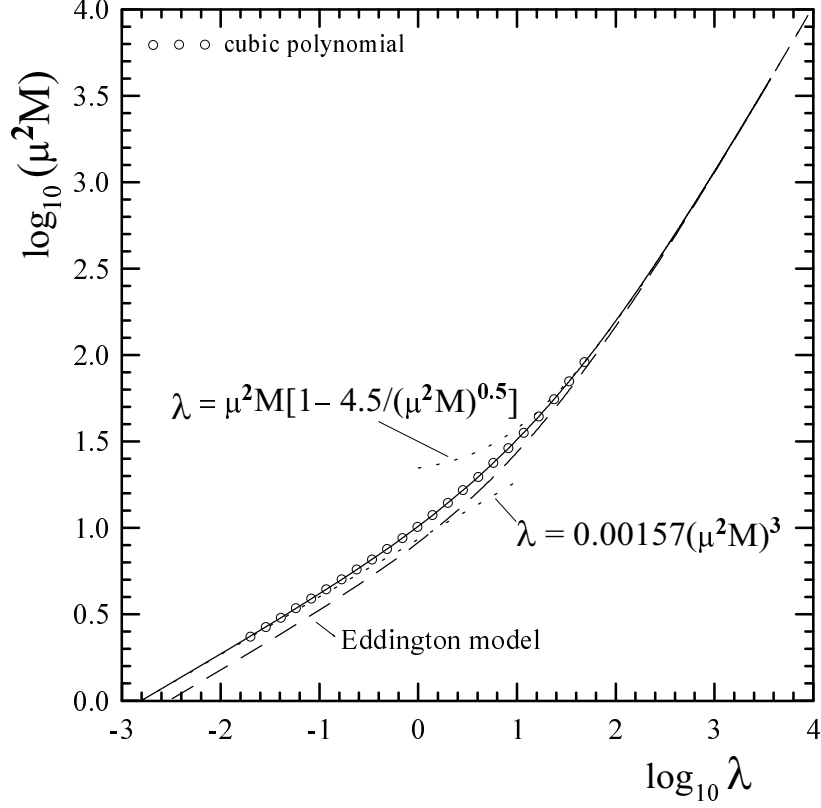


Figure 8: The mass-luminosity relation (M in M_{\odot} , see text).

Figure 7 shows luminosity L_0 in terms of L_{Ed} as a function of $\mu^2 M$ [solid curve specified by Eq. (24)]. The curve virtually holds for all the three energy generation modes — a small difference for the pp-chain at $\mu^2 M < 10$ is indistinguishable on the scale of the figure. For given $\mu^2 M$, the Eddington model is always over-luminous (by a factor of two at $\mu^2 M < 10$).

For the sake of practical use, it is worth to rewrite the mass-luminosity relation in terms of variable λ :

$$\lambda \equiv \mu^2 \frac{M}{M_{\odot}} \frac{L_0}{L_{\text{Ed}}} = \frac{\mu^2 \kappa_0 L_0}{4\pi c G M_{\odot}} = 1.5426 \times 10^{-5} \mu^2 (1 + X) \frac{L_0}{L_{\odot}}, \quad (34)$$

Connecting the asymptotics for small and large $\mu^2 M$ -values by a cubic spline that ensures the continuity of the function and its first derivatives (open

Table 2: Integral properties of selected models

$\mu^2 M$	0	10	30	100	300	1000	4000	Edd
E_g^*	-1.227	-1.206	-1.205	-1.254	-1.318	-1.383	-1.435	-1.5
E_T	0.6137	0.6969	0.8350	1.016	1.166	1.292	1.387	1.450
I^\dagger	0.1561	0.1616	0.1630	0.1536	0.1412	0.1302	0.1222	0.113
I_{conv}	0.0139	0.0439	0.0908	0.1247	0.1309	0.1271	0.1214	—
t_s	2.438	2.517	2.580	2.624	2.649	2.665	2.677	2.723
t_{conv}	0.269	0.433	0.619	0.843	1.044	1.251	1.472	—
τ_c	1.441	1.426	1.475	1.664	1.896	2.132	2.329	2.587
$\langle \gamma \rangle$	5/3	1.532	1.453	1.401	1.3733	1.3555	1.3445	1.345
ω	2.804	2.109	1.629	1.288	1.058	0.840	0.627	0.667

* E_g attains a maximum -1.2005 at $\mu^2 M = 18.5$

† I attains a maximum 0.1636 at $\mu^2 M = 21$

circles in Fig. 8) one obtains the following analytical approximation:

$$\begin{aligned}
 \lg(\mu^2 M) &= 0.9347 + \frac{1}{3} \lg \lambda, & (\lg \lambda \leq -1.7), \\
 \lg(\mu^2 M) &= 1.015209 + 0.449843 \lg \lambda + 0.0534969 \lg^2 \lambda & (35) \\
 &\quad + 0.00754094 \lg^3 \lambda, & (-1.7 < \lg \lambda < 1.7), \\
 \mu^2 M &= 10.125 \left(1 + 0.0987654 \lambda + \sqrt{1 + 0.1975 \lambda} \right), & (\lg \lambda \geq 1.7).
 \end{aligned}$$

Equation (35) allows to estimate M when the luminosity L_0 and the representatives of composition (μ and X) are known. On the contrary, in order to estimate L_0 for given M and composition one can either solve Eq. (35) for λ or use the following accurate approximation:

$$\begin{aligned}
 \lambda &= 0.00157 (\mu^2 M)^3, & (\mu^2 M \leq 2.4), \\
 \lg \lambda &= -2.907029 + 3.552793 \lg(\mu^2 M) - 0.7717945 \lg^2(\mu^2 M) & (36) \\
 &\quad + 0.078623 \lg^3(\mu^2 M), & (2.4 < \mu^2 M < 100), \\
 \lambda &= \mu^2 M \left(1 - \frac{4.5}{\sqrt{\mu^2 M}} \right), & (\mu^2 M \geq 100).
 \end{aligned}$$

Concluding this section we present in Table 2 a number of integral properties of stellar models such as gravitational E_g and thermal E_T energies (in

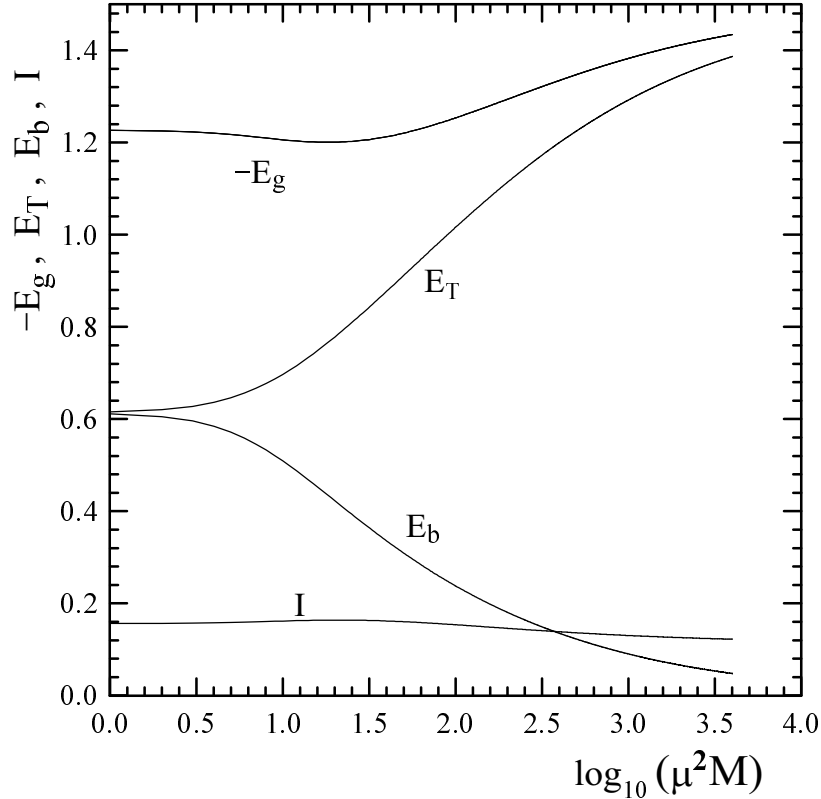


Figure 9: Dimensionless gravitational E_g and thermal E_T energies, central moment of inertia I , and gravitational binding energy E_b versus $\mu^2 M$.

units GM^2/R), central moment of inertia of the whole star $I = \int_0^M r^2 dm$ and that of the convective core I_{conv} (in units MR^2), the time sound takes to propagate from the center up to the surface $t_s = \int_0^R \frac{dr}{\sqrt{\gamma P/\rho}}$ and to the convective core boundary t_{conv} (in units $\sqrt{R^3/(GM)}$), column density of the star $\tau_c = \int_0^R \rho dr$ (in units M/R^2), average adiabatic index $\langle \gamma \rangle = \frac{\int_0^M \gamma (P/\rho) dm}{\int_0^M (P/\rho) dm}$, and an estimate of fundamental angular frequency $\omega = \sqrt{(3\langle \gamma \rangle - 4)|E_g|/I}$ of radial pulsations (in units $\sqrt{GM/R^3}$).

The last column in Table 2 presents the properties of the Eddington standard model at $\mu^2 M = 4000$. Note that for the standard model the dimensionless E_g , I and τ_c are determined by the polytrope $n = 3$ structure and do not depend on $\mu^2 M$.

Figure 9 shows E_g , E_T , I , and gravitational binding energy $E_b = -E_{\text{tot}} = -(E_g + E_T)$ as functions of $\mu^2 M$.

4 Comparison with detailed models

In order to demonstrate potentialities of the similarity theory we compare our results with detailed models of massive main sequence stars calculated by Schaller et al. (1992) and the models of helium and carbon-oxygen stars (Wolf-Rayet stars) studied by Langer (1989) and Deinzer and Salpeter (1964). Figures 10–13 display such a comparison. Solid curves in Fig. 10 are obtained

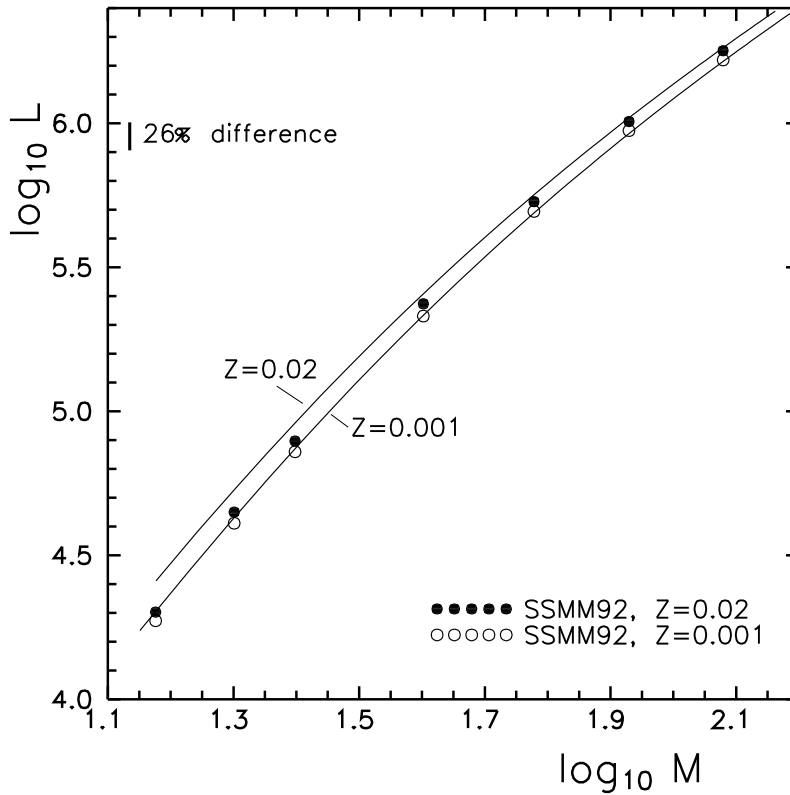


Figure 10: The mass-luminosity relation (solid lines) in comparison with the detailed models of Schaller et al. (1992) (filled and open circles). M and L are in solar units.

with the aid of Eq. (36) for two specified by Schaller et al. (1992) compo-

sitions: $X=0.680$, $Y=0.300$, $Z=0.020$ (upper curve) and $X=0.756$, $Y=0.243$, $Z=0.001$ (lower curve). One can observe an excellent agreement for low metallicity ($Z = 0.001$) and a fairly good coincidence for $Z = 0.02$. In the latter case our models are slightly over-luminous (by 25% at $M = 15 M_{\odot}$). This natural result can be interpreted as on average a 25% contribution to the opacity coming from sources other than the electron scattering.

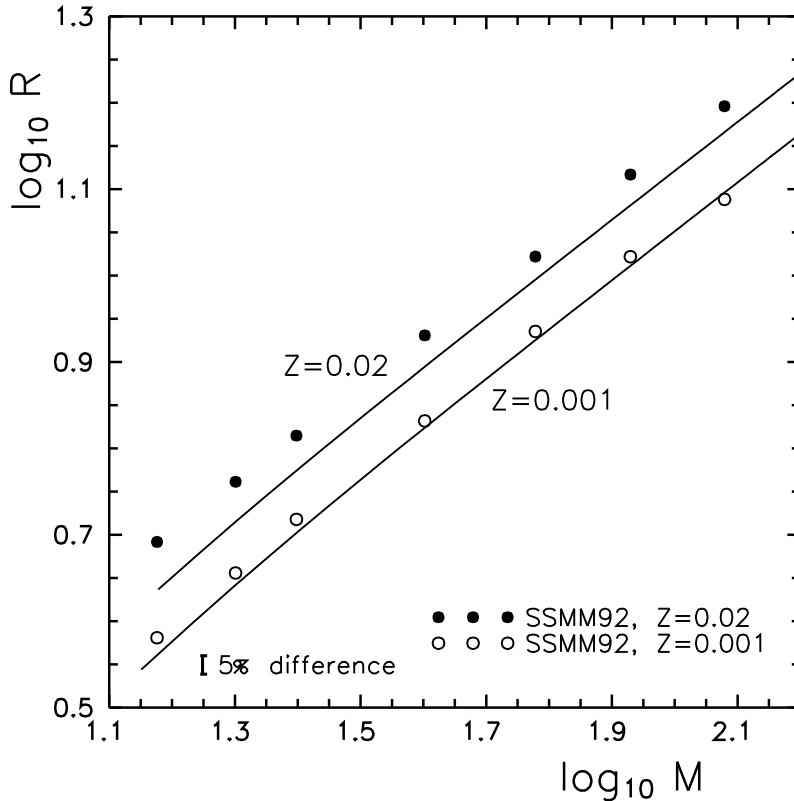


Figure 11: The mass-radius relation (solid lines) in comparison with the detailed models of Schaller et al. (1992) (filled and open circles). M and R are in solar units.

The mass-radius relation for the same models is shown in Fig. 11. The detailed models have systematically larger radii (typically by $\sim 5\%$ for $Z=0.02$) as compared with our models (solid lines). This can be explained by a noticeable increase in opacity in stellar envelope owing to the absorption in atomic spectral lines (Imshennik, Nadyozhin, 1967). The solid lines were calculated with the aid of Eqs. (32) and (33) assuming the CNO-cycle as the

main energy source with the energy generation law taken from Caughlan, Fowler (1988) and approximated by

$$\varepsilon_{\text{CNO}} = 8.43 \times 10^{-3} X_{\text{CNO}} X \rho T_7^{16} \text{ erg g}^{-1} \text{ s}^{-1}, \quad (2.2 \leq T_7 \leq 3.6), \quad (37)$$

where $T_7 \equiv T/10^7 \text{K}$ and ρ is in g cm^{-3} . Within the indicated limits for T_7 , the accuracy of Eq. (37) is better than 10%.

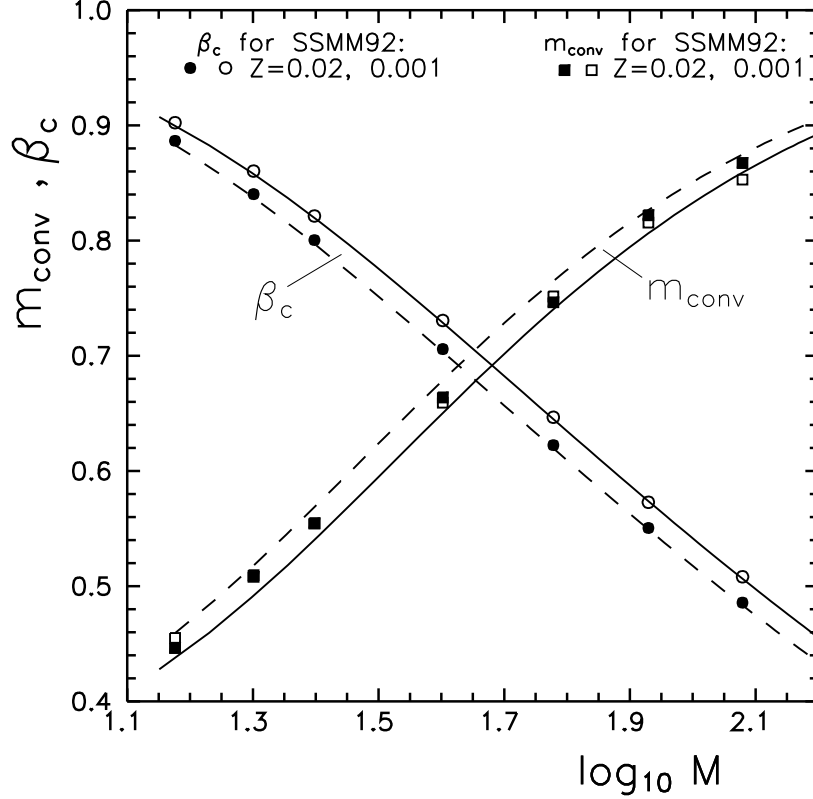


Figure 12: Dimensionless mass of the convective core m_{conv} and central value of β (solid and dashed lines) in comparison with Schaller et al. (1992) (filled and open circles and squares). Solid and dashed lines are for $Z = 0.001$ and $Z = 0.02$, respectively; M is in M_{\odot} .

Similar approximation for the 3α -reaction is given by the following power law

$$\varepsilon_{3\alpha} = 4.95 \times 10^{-38} Y^3 \rho^2 T_7^{30} \text{ erg g}^{-1} \text{ s}^{-1}, \quad (T_7 > 8). \quad (38)$$

The accuracy of the approximation is better than 10% at $T_7 > 8$.

The structural properties of our models are also in a good agreement with the detailed models as it is exemplified in Fig. 12 for central value of β and the convective core mass fraction m_{conv} .

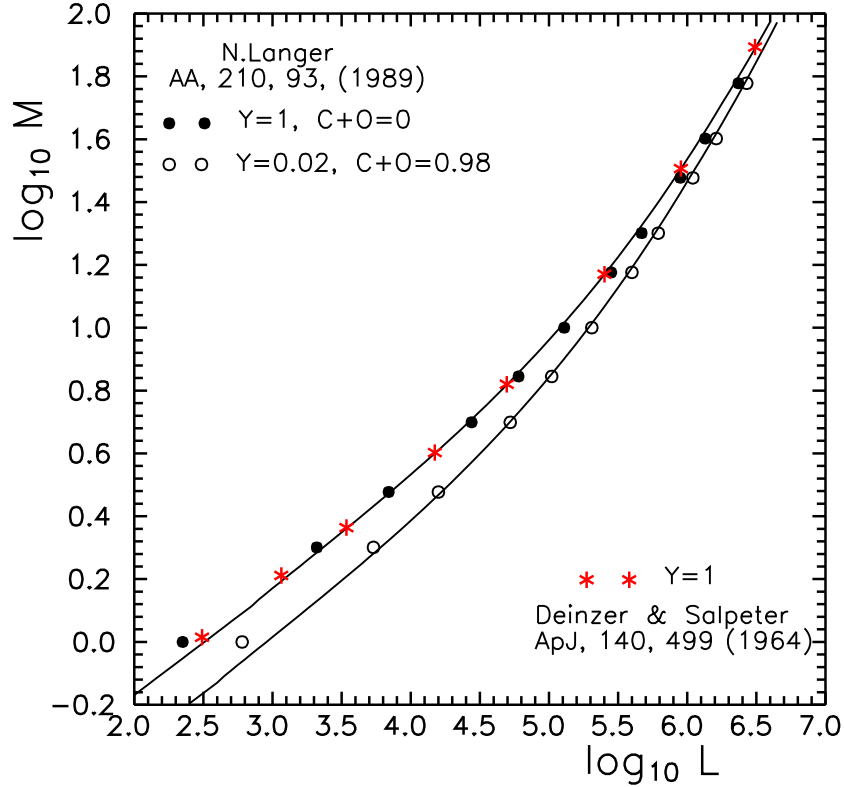


Figure 13: The mass-luminosity relation for the helium and carbon-oxygen Wolf-Rayet stars (solid lines) in comparison with the detailed models of Langer (1989) (filled and open circles) and Deinzer and Salpeter (1964) (asterisks). M and L are in solar units.

Figure 13 shows the mass-luminosity relation for pure helium stars ($Y=1$) calculated by Deinzer and Salpeter (1964) and Langer (1989), and for carbon-oxygen Wolf-Rayet stars, with the mass fractions of carbon, oxygen, and helium $X_C=0.113, X_O=0.867, Y=0.02$, respectively (Langer, 1989), in comparison with the mass-luminosity relation for our models determined by Eq. (35) (solid lines). One has to specify the hydrogen mass fraction $X=0$ in Eq. (34) for λ and make use of the following expression for the mean molecular mass

μ :

$$\mu = \frac{48}{36Y + 28X_C + 27X_O}, \quad (Y + X_C + X_O = 1). \quad (39)$$

Our results are in a very good agreement with the detailed models even for such a small mass as $1 M_\odot$.

5 Discussion and conclusions

It is interesting to apply the mass-luminosity relation given by Eqs. (35) and (36) to the very massive stars observed in the Milky Way, in Magellanic Clouds and in a number of nearby resolved galaxies. There exist comprehensive observational data for several dozens of such stars (see, for instance, Figer et al., 1998; Puls et al., 1996; Humphreys, Davidson, 1994; Sandage, Tammann, 1974). A detailed analysis of the efficiency of the similarity theory in deriving the properties of such stars from observations is in need of a special paper. Here as an example we consider the Pistol star studied in detail by Figer et al. (1998). Assuming that the star was initially of solar composition ($X=0.707$, $Y=0.274$, $Z=0.019$; Anders, Grevesse, 1989) and had the luminosity $L_0 = 10^{6.7 \pm 0.5} L_\odot$ (Najarro, Figer, 1999), one can estimate from Eq. (35) its initial mass to be $M = 116, 246, \text{ and } 595 M_\odot$ for $L_0 = 10^{6.2}, 10^{6.7}, \text{ and } 10^{7.2} L_\odot$, respectively. The corresponding initial radii derived from Eqs. (32) and (33) turn out to be $R = 14, 22, \text{ and } 36 R_\odot$ for the CNO energy generation rate given by Eq. (37). The range of masses ($116 - 595 M_\odot$) corresponds to the range ($44 - 230$) in the parameter $\mu^2 M$ since $\mu = 0.618$ for the solar composition. Such stars have luminosity of $(0.4 - 0.7)L_{\text{Ed}}$ (Fig. 7) and very large convective cores: $m_{\text{conv}} = 0.86 - 0.976$ [Eq. (30) or Fig. 5]. Estimating the Pistol star initial mass we have implied that its luminosity has not changed appreciably during the evolution. The star seems to be in a state close to the exhaustion of hydrogen in the convective core — i.e., it is about to leave the Main Sequence. According to Schaller et al. (1992), an increment in the luminosity ΔL_0 within the Main Sequence strip decreases with increasing mass M . Since for $M = 120 M_\odot$ (solar metallicity) $\Delta L_0 \approx 25\%$, initially the Pistol star might have been by $\sim 10\%$ less massive than the estimates stated above.

The properties of stellar structure obtained here are in a fair agreement also with the detailed models of the very massive, $(100 - 250) M_\odot$, initially zero-metallicity Pop III stars calculated in the UCSC astrophysical group

(Woosley, 2005), especially when the stars are definitely settled at their Main Sequence in the state of thermal equilibrium.

The similarity theory of the structure of very massive stars formulated here allows to obtain the following important results:

1. A simple approximation formula for the mass-luminosity relation, given by Eqs. (34), (35), and (36), is valid for different chemical compositions and virtually does not depend on the energy generation mode (pp-chain, CNO-cycle, or 3α -reaction).
2. The overall structure of very massive stars, described in dimensionless variables listed in Eq. (11), depends only on the parameter $\mu^2 M$ where μ is the mean molecular mass. Practically, this structure turns out to be independent of the energy generation mode — be it the CNO-cycle, 3α -reaction, or pp-chain.
3. Although with increasing $\mu^2 M$ the stellar structure approaches that of the Eddington standard model, the convergence proves to be rather slow. Even for $\mu^2 M = 4000$ there are still noticeable discrepancies in some stellar parameters. For instance, the central dimensionless pressure and density are respectively by about 20% and 15% lower than for the Eddington model (Fig. 4).

Acknowledgements

One of us (DKN) has a pleasure to thank the Max-Planck-Institut für Astrophysik for financial support and hospitality. The work was partly supported by the Russian Foundation for Basic Research (project no. 04-02-16793-a).

References

- Anders E., Grevesse N.
Geochim. Cosmochim. Acta 1989, **53**, 197.
- Biermann L. Zs. für Astrophysik 1931, **3**, 116.
- Caughlan, G.R., Fowler, W.A.
Atomic Data Nucl. Data Tables 1988, **40**, 283.

- Chandrasekhar S. *An Introduction to the Study of Stellar Structure*, Chicago: Univ. of Chicago Press, 1939.
- Chiu H.-Y. *Stellar Physics*, vol. 1, Blaisdell Pub., Massachusetts-Toronto-London, 1968.
- Cowling T.G. Mon. Not. RAS 1934, **94**, 768.
- Cox J.P., Guili R.T. *Principles of stellar structure*, vol. 2, Gordon and Breach, New York, 1968.
- Deinzer W., Salpeter E.E. *Astrophys. J.* 1964, **140**, 499.
- Dibai E.A., Kaplan S.A., *Razmernosti i podobie astrofizicheskikh velichin* (Dimensions and similarity of astrophysical quantities), Nauka Pub., Moscow, 1976 (in Russian).
- Eddington A.S. *The Internal Constitution of the Stars*, Cambridge, 1926.
- Figer D.F., Najarro F., Morris M., McLean I.S., Gerralde T.R., Ghez A.M., Langer N. *Astrophys. J.* 1998, **506**, 384.
- Henrich L.R. *Astrophys. J.* 1943, **98**, 192.
- Humphreys R.M., Davidson K. *Publ. Astron. Soc. Pacific* 1994, **106**, 1025.
- Imshennik V.S., Nadyozhin D.K. *Astron. Zh.* 1967, **44**, 377. (Sov. Astr. 1967, **11**, 297).
- Imshennik V.S., Nadyozhin D.K. *Astron. Zh.* 1968, **45**, 81. (Sov. Astr. 1968, **12**, 63).
- Kippenhahn R., Weigert A. *Stellar structure and evolution*, Springer-Verlag, Berlin-Heidelberg, 1990.
- Langer N. *Astron. Astrophys.* 1989, **210**, 93.
- Najarro F., Figer D.F. *Astrophys. Space Sci.* 1999, **263**, 251.
- Naur P., Osterbrock D.E. *Astrophys. J.* 1953, **117**, 306.

Puls J., Kudritzki R.-P., Herrero A., et al.
Astron. Astrophys. 1996, **305**, 171.

Sandage A., Tammann G.A. *Astrophys. J.* 1974, **191**, 603.

Schaller G., Schaerer D., Meynet G., Maeder A.
Astron. Astrophys. Suppl. 1992, **96**, 269.

Schwarzschild M. *Structure and Evolution of Stars*,
Princeton Univ. Press, Princeton, New Jersey, 1958.

Sedov L.I. *Similarity and dimensional methods in mechanics*
Academic Press, New York, 1959 (4th Russian ed.). See also
the 8th revised edition, Nauka Pub., Moscow, 1977 (in Russian).

Strömgren B. *Handbuch der Astrophysik* 1936, **7**, 121.

Woolley S.E. 2005, private communication.